

# Polymer Masked–Unmasked Protein Therapy: Identification of the Active Species after Amylase Activation of Dextrin–Colistin Conjugates

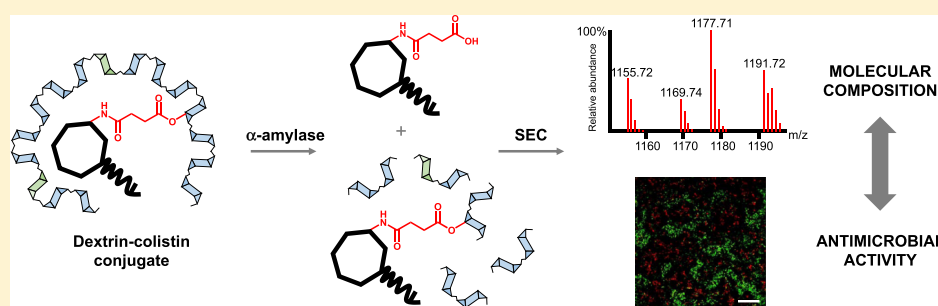
Mathieu Varache,<sup>†</sup> Lydia C. Powell,<sup>†</sup> Olav A. Aarstad,<sup>‡</sup> Thomas L. Williams,<sup>§</sup> Margot N. Wenzel,<sup>§</sup> David W. Thomas,<sup>†</sup> and Elaine L. Ferguson<sup>\*,†</sup>

<sup>†</sup>Advanced Therapies Group, Oral and Biomedical Sciences, School of Dentistry, College of Biomedical and Life Sciences, Cardiff University, Heath Park, Cardiff CF14 4XY, U.K.

<sup>‡</sup>Department of Biotechnology and Food Sciences, Norwegian University of Science and Technology, Trondheim 7491, Norway

<sup>§</sup>School of Chemistry, Cardiff University, Main Building, Park Place, Cardiff CF10 3AT, U.K.

## Supporting Information



**ABSTRACT:** Polymer masked–unmasked protein therapy (PUMPT) uses conjugation of a biodegradable polymer, such as dextrin, hyaluronic acid, or poly(L-glutamic acid), to mask a protein or peptide’s activity; subsequent locally triggered degradation of the polymer at the target site regenerates bioactivity in a controllable fashion. Although the concept of PUMPT is well established, the relationship between protein unmasking and reinstatement of bioactivity is unclear. Here, we used dextrin–colistin conjugates to study the relationship between the molecular structure (degree of unmasking) and biological activity. Size exclusion chromatography was employed to collect fractions of differentially degraded conjugates and ultraperformance liquid chromatography–mass spectrometry (UPLC–MS) employed to characterize the corresponding structures. Antimicrobial activity was studied using a minimum inhibitory concentration (MIC) assay and confocal laser scanning microscopy of LIVE/DEAD-stained biofilms with COMSTAT analysis. In vitro toxicity of the degraded conjugate was assessed using an 3-(4,5-dimethylthiazol-2-yl)-2,5-diphenyl tetrazolium bromide assay. UPLC–MS revealed that the fully “unmasked” dextrin–colistin conjugate composed of colistin bound to at least one linker, whereas larger species were composed of colistin with varying lengths of glucose units attached. Increasing the degree of dextrin modification by succinylation typically led to a greater number of linkers bound to colistin. Greater antimicrobial and antibiofilm activity were observed for the fully “unmasked” conjugate compared to the partially degraded species (MIC = 0.25 and 2–8 μg/mL, respectively), whereas dextrin conjugation reduced colistin’s in vitro toxicity toward kidney cells, even after complete unmasking. This study highlights the importance of defining the structure–antimicrobial activity relationship for novel antibiotic derivatives and demonstrates the suitability of LC–MS to aid the design of biodegradable polymer–antibiotic conjugates.

**KEYWORDS:** colistin, polymer therapeutics, mass spectrometry, infection, Gram-negative bacteria

## 1. INTRODUCTION

The emergence of antibiotic-resistant bacteria represents a major global health threat and a significant clinical and societal challenge. Of particular concern is the rapidly increasing resistance rate of many Gram-negative bacterial pathogens, which has been mirrored by a decrease in research and development of new antibiotic compounds.<sup>1</sup> In 2018, the World Health Organization (WHO) published a list of pathogens posing the greatest threat to human health.<sup>2</sup> The most critical pathogen group includes *Pseudomonas aeruginosa*,

*Acinetobacter baumannii*, and Enterobacteriaceae (which includes *Klebsiella pneumoniae* and *Escherichia coli*) because of high levels of drug resistance and severity of infection in hospitals, nursing homes, and among critically ill and elderly patients.

**Received:** April 10, 2019

**Revised:** May 21, 2019

**Accepted:** May 24, 2019

**Published:** May 24, 2019

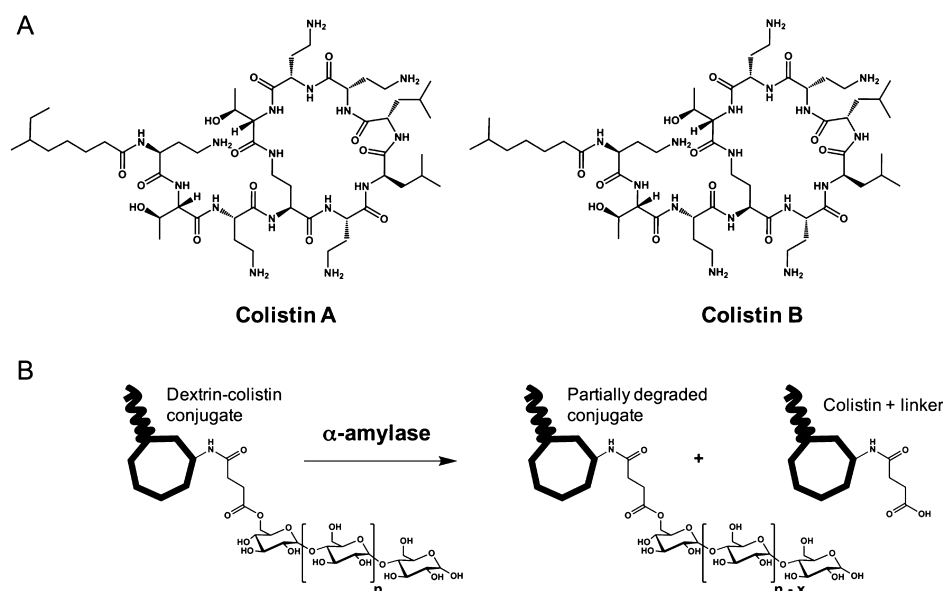


**Figure 1.** (A) Chemical structure of the two subgroups of colistin. (B) Schematic representation of the degradation of the dextrin–colistin conjugate by  $\alpha$ -amylase. Amylase hydrolyzes dextrin at random locations along its chain to yield the disaccharides maltose and iso-maltose, resulting in a decrease in dextrin’s chain length by  $x$  D-glucose units, where  $n$  is the DP of the polymer.

Although progress remains to be made in the development of new classes of antibiotics, older “drugs of last resort” such as colistin are increasingly being employed<sup>3,4</sup> as, despite higher incidences of toxicity and significant long-term complications, they have retained antimicrobial efficacy. Colistin (also known as polymyxin E) is a cationic peptide from the polymyxin family of antibiotics. It was isolated from *Bacillus colistinus* in 1947 and has been on the market as a treatment for Gram-negative bacterial infections since 1950.<sup>5</sup> Several years later, however, reports of dose-limiting nephro- and neurotoxicity forced clinicians to cease using this potent antibiotic.<sup>6,7</sup> Colistin comprises a cyclic heptapeptide and tripeptide side chain acylated at the N-terminus by a fatty acid. Commercially available colistin contains at least 30 different components, 13 of which have been isolated and identified.<sup>8,9</sup> The major components are colistin A (polymyxin E1) and colistin B (polymyxin E2) which, together, account for more than 85% of the total weight of the raw material (Figure 1A).<sup>10</sup> The two substances differ in the length of the fatty acid side chain by one methylene group.

We have recently employed polymer masked–unmasked protein therapy (PUMPT) to deliver colistin conjugated to dextrin using nonspecific carbodiimide conjugation chemistry.<sup>11</sup> PUMPT uses conjugation of a biodegradable polymer, such as dextrin, hyaluronic acid, or poly(L-glutamic acid), to mask a protein or peptide’s activity.<sup>12–14</sup> Following intravenous administration, colistin is expected to localize and accumulate within sites of inflammation by the enhanced permeability and retention (EPR) effect,<sup>11,15,16</sup> where the antibiotic can be released from the conjugate via amylase-triggered degradation of dextrin. Reinstatement of the payload’s biological activity may be controlled by employing dextrans of different molecular weights and degrees of modification, tailoring the conjugation chemistry and by the degree of inflammation/enzymatic activity at the “target” site.<sup>11,14</sup> In contrast to the administration of growth factors to induce healing,<sup>17</sup> anti-infective therapy requires rapid delivery of the antibacterial payload at the site of infection. Previous

studies of dextrin–colistin conjugates have attempted to optimize dextrin–colistin conjugate’s release kinetics by varying the molecular weight and degree of succinylation of dextrin.<sup>11</sup> Ferguson et al. demonstrated that conjugates containing 7500 g/mol dextrin with 1 mol % succinylation resulted in the release of ~80% of the bound drug within 48 h when incubated with physiological levels of amylase (100 IU/L).<sup>11</sup> Dextrin–colistin conjugates exhibited reduced in vitro and in vivo toxicity and prolonged plasma half-life (dextrin–colistin  $t_{1/2}$  = 135 min, colistin  $t_{1/2}$  = 53 min).<sup>11</sup> Sustained, concentration-dependent killing of *A. baumannii* was observed in an in vitro pharmacokinetic–pharmacodynamic model, and unmasking of the conjugate in human wound exudate was confirmed.<sup>15</sup> The conjugates also demonstrated antibacterial activity (against Gram-negative pathogens) similar to the commercially available prodrug, colistin methanesulfonate (CMS, Colomycin). Interestingly, however, even after complete unmasking, antimicrobial activity remained lower than the unmodified drug; being more pronounced in conjugates containing dextrin with higher degrees of modification.<sup>11</sup>

Whilst the concept of PUMPT is well established, the degree to which unmasking must occur to completely reinstate the payload’s bioactivity has not yet been determined. In the dextrin–colistin conjugate model,  $\alpha$ -amylase randomly cleaves the dextrin backbone, yielding the disaccharides, maltose and iso-maltose.<sup>18</sup> The dextrin is, however, attached to colistin via a nondegradable amide bond; therefore, even after complete degradation of dextrin, substituent groups will remain attached to colistin (Figure 1B). Their presence may explain the inability to completely reinstate antibiotic activity following exposure to amylase. In the present work, we hypothesize that these remaining substituent groups, particularly the number of glucose units, may strongly affect antimicrobial properties of the unmasked conjugate. Here, the chemical composition of differentially degraded dextrin–colistin conjugates is reported and related to the species’ biological activity and in vitro toxicity, to determine the optimal extent of conjugate

unmasking that is required to achieve maximal antimicrobial activity.

## 2. MATERIALS AND METHODS

**2.1. Materials.** Type I dextrin from corn ( $M_w = 7500$  g/mol), colistin sulfate,  $\alpha$ -amylase from human saliva, *N*-hydroxysulfosuccinimide (sulfo-NHS), 3-(4,5-dimethylthiazol-2-yl)-2,5-diphenyl tetrazolium bromide (MTT), bicinchoninic acid (BCA) solution, and dimethyl sulfoxide (DMSO) maltose oligomers [degree of polymerization (DP) 2, 3, 6, and 7] were purchased from Sigma-Aldrich (Poole, U.K.). 1-Ethyl-3-(3-(dimethylamino)propyl carbodiimide hydrochloride) (EDC) was acquired from Pierce (Rockford, USA). Disodium hydrogen phosphate, potassium dihydrogen phosphate, potassium chloride, 4-dimethylaminopyridine, and sodium chloride were from Fisher Scientific (Loughborough, U.K.). Pullulan gel filtration standards ( $M_w = 11\ 800$ – $210\ 000$  g/mol) were purchased from Polymer Laboratories (Church Stretton, U.K.). Unless otherwise stated, all chemicals were of analytical grade and used as received. All solvents were of general reagent grade (unless stated) and were from Fisher Scientific (Loughborough, U.K.).

**2.2. Bacterial Culture.** Bacterial colonies were grown on blood agar supplemented with 5% horse blood, and liquid cultures were suspended in a tryptone soya broth for overnight culture or Mueller–Hinton broth (MHB) for minimum inhibitory concentration (MIC) determination (Oxoid; Basingstoke, U.K.). Antibacterial activity was screened against an *E. coli* clinical isolate (VS) provided by Professor Timothy Walsh (Department of Infection and Immunity, Cardiff University). Its known relevant genotype and origin have been described by Khan et al.<sup>19</sup>

**2.3. Cell Culture.** Human kidney proximal tubule cells (HK-2) were obtained from ATCC (Manassas, USA) and screened to be free of mycoplasma contamination before use. Keratinocyte serum-free medium (K-SFM) with L-glutamine, epidermal growth factor (EGF), bovine pituitary extract (BPE), and 0.05% w/v trypsin-0.53 mM ethylenediaminetetraacetic acid were obtained from Invitrogen Life Technologies (Paisley, U.K.).

**2.4. Synthesis of Dextrin–Colistin Conjugates.** Dextrin–colistin conjugates were synthesized using EDC and sulfo-NHS and characterized as previously described.<sup>11</sup> The dextrin–colistin conjugate used in these studies contained dextrin ( $M_w = 7500$  g/mol; DP = 50) with 1 mol % succinylation, a colistin content of 7.6% w/w (by BCA assay) (equivalent to 2 dextrin chains per colistin), and a molecular weight of 10 000 g/mol (by gel permeation chromatography with pullulan standards,  $M_w/M_n = 1.5$ ). Free colistin content, analyzed by fast protein liquid chromatography (LC), was determined as <4%. The characteristics of dextrin–colistin conjugates used to analyze the effect of succinylation on the degree of peptide modification are summarized in Table S1.

**2.5. Amylase Degradation of Dextrin–Colistin Conjugates.** Unmasked dextrin–colistin conjugates were prepared by incubation of the dextrin–colistin conjugate (3 mg/mL colistin base in PBS, pH 7.4) with amylase (100 IU/L) for up to 48 h at 37 °C. Samples were subsequently lyophilized and stored at –20 °C prior to analysis.

**2.6. Analysis of Masked–Unmasked Conjugates and Fractionation by SEC.** Samples (10–100 mg) were dissolved in 4 mL of 0.1 M ammonium acetate (pH 6.9, 0.22  $\mu$ m filter-sterilized) and then manually injected into an 8 mL sample

loop. The size exclusion chromatography (SEC) system consisted of 3 serially connected HiLoad Superdex 30 columns ( $2.6 \times 60$  cm), a Shimadzu LC-10 AD vp pump, a Shimadzu SPD-10 AV vp UV-detector (215 nm), and a Shodex RI-101 refractive index detector. Data were collected with an Adam view 4561 converter and a 4017P input module. Samples were eluted at a flow rate of 0.8 mL/min and fractions collected every 50 min between 400 and 800 min and stored at –20 °C until lyophilization. Lyophilized samples were dissolved in MQ water and then freeze-dried ( $\times 5$ ) to remove ammonium acetate. Total protein content of the degraded fractions was determined by the BCA assay using colistin standards.

**2.7. Characterization of the Collected Fractions by LC–Mass Spectrometry.** Colistin (10  $\mu$ g/mL, 5  $\mu$ L) and fractions (1 mg/mL total weight, 5  $\mu$ L) were analyzed on a Synapt G2-Si quadrupole time-of-flight (QTOF) mass spectrometer (Waters, UK) operating in the positive electrospray ionization mode, coupled to an ACQUITY H-Class UPLC system (Waters, UK). Separation was performed using an ACQUITY UPLC CSH C18 column (300 Å, 1.7  $\mu$ m, 2.1  $\times$  100 mm, Waters) held at 40 °C with a flow rate of 0.3 mL/min. A multistep gradient method using 98% A for 2 min followed by a linear gradient to 50% A for 18 min, where A is water (0.1% formic acid) and B is acetonitrile (0.1% formic acid).

**2.8. Analysis of Unmasked Conjugate by High-Performance Anion Exchange Chromatography with Pulsed Amperometric Detection.** Samples (0.1–1 mg/mL total weight) were analyzed using a Dionex ICS-5000+ ion chromatography system (Thermo Scientific, Oslo, Norway) with an electrochemical detector fitted with a nondisposable gold working electrode. Samples were injected via a 25  $\mu$ L loading loop. Separation was performed using a CarboPac PA-100 (4  $\times$  50 mm, Dionex) guard column and CarboPac PA-100 (4  $\times$  250 mm, Dionex) analytical column connected held at 24 °C with a flow rate of 1 mL/min. Analysis was performed using isocratic 100 mM sodium hydroxide and a linear sodium acetate gradient from 10 to 610 mM in 90 min. A Carboquad waveform was used for detection. Data were collected and processed using Chromeleon 7.2 software.

**2.9. Measurement of Antimicrobial Activity.** Antimicrobial activity was measured using broth microdilution in a standard MIC assay.<sup>20</sup> *E. coli* strain, VS, was suspended in MHB (100  $\mu$ L, 1 to  $5 \times 10^4$  CFU/mL) and incubated in 96-well microtiter plates in serial twofold dilutions of the test compounds. To prepare initial dilutions, samples were dissolved in PBS at 50  $\mu$ g/mL (colistin base) and then diluted in MHB to a starting concentration of 16  $\mu$ g/mL colistin. Experiments were performed in triplicate and expressed as the modal value.

**2.10. Bacterial Growth Curves.** The pharmacokinetic profile of individual fractions was studied against *E. coli*. Colistin and the derived fractions (with 4  $\mu$ g/mL starting colistin concentration) were added to 96-well microtiter plates in serial twofold dilutions. Plates were wrapped in Parafilm M and placed in a microtiter plate reader at 37 °C; bacterial growth was assessed by measuring absorbance (at 600 nm), hourly, for 48 h. The absorbance values were expressed as mean  $\pm$  standard deviation (SD) ( $n = 3$ ).

**2.11. Confocal Laser Scanning Microscopy and COMSTAT Analysis.** The direct effects of the analytes were studied using confocal laser scanning microscopy (CLSM) imaging. *E. coli* biofilms were grown in Grenier 96-well glass-

bottomed plates in MHB  $\pm$  colistin or degraded fractions. A 1:10 inoculum of *E. coli* overnight culture ( $1 \times 10^7$  CFU/mL) was used, and plates were incubated at 37 °C for 24 h. The supernatant was carefully removed from the plates, and the biofilms were stained with LIVE/DEAD (Baclight Bacterial Viability Kit, Molecular Probes) for 10 min before imaging using a Leica SP5 CLSM. CLSM images were achieved with a  $\times 63$  lens (oil) and a step size of 0.79  $\mu\text{m}$ . The resultant CLSM z-stack images were analyzed using COMSTAT image analysis software for quantification of three-dimensional biofilm structures through measurement of biomass, mean biofilm thickness, roughness coefficient, and DEAD/LIVE bacterial ratio.<sup>21</sup> Statistical calculations were performed using Minitab v.14 (Minitab, State College, PA). To determine significant differences for pair-wise comparisons, the nonparametric data were analyzed using the Mann–Whitney test. A *p* value < 0.05 was considered statistically significant.

**2.12. In Vitro Cytotoxicity.** An MTT assay was used to assess cell viability in a human kidney (HK-2) cell line (72 h incubation). HK-2 cells (passages P15 to P20) were seeded into sterile 96-well microtiter plates ( $2.5 \times 10^4$  cells/mL) in 0.1 mL/well of media (K-SFM) containing L-glutamine, EGF, and BPE and allowed to adhere for 24 h. The medium was then removed, and test compounds were added to the wells. To study the effect of colistin sulfate, fraction F8, and intact dextrin–colistin conjugate on cell viability, complete media were supplemented with a range of different concentrations of each. After a further 67 h incubation, MTT (20  $\mu\text{L}$  of a 5 mg/mL solution in PBS) was added to each well and incubated for a further 5 h. The medium was then removed, and the precipitated formazan crystals solubilized by the addition of optical grade DMSO (100  $\mu\text{L}$ ). After 30 min, the absorbance of each well was measured at 540 nm using a microtiter plate reader. Cell viability was expressed as a percentage of the viability of untreated control cells and expressed as mean  $\pm$  standard error of the mean (SEM) ( $n = 18$ ). Evaluation of significance was achieved using a two-way analysis of variance (ANOVA) followed by Bonferroni post hoc tests that correct for multiple comparisons. All statistical calculations were performed using a GraphPad Prism, version 6.0h for Macintosh, 2015.

### 3. RESULTS

**3.1. Chemical Characterization of Degraded Fractions.** SEC-RI of the dextrin–colistin conjugate after amylase unmasking showed a decrease of the peak corresponding to the conjugate (400–750 min) (Figure 2A). This was mirrored by the appearance of a peak corresponding to a species with a molecular weight close to that of colistin (retention time  $\sim 760$  min), which was also observed by SEC-UV (Figure 2B). SEC-RI revealed peaks corresponding to water, ammonium acetate salts, and glucose ( $\sim 1000$  min), whereas added sodium chloride and phosphate salts eluted at  $\sim 1050$  min. Several oligosaccharides, released by the degradation of dextrin, were also observed (850–950 min). High-performance anion exchange chromatography with pulsed amperometric detection (HPAEC-PAD) revealed that the most intense peaks corresponded to maltose (DP = 2) and maltotriose (DP = 3) (Figure S1). Therefore, assuming that the intensity of the peaks observed by HPAEC-PAD mirrored those observed by SEC-RI, the two major peaks observed by the latter at 926 and 951 min were identified as maltotriose and maltose, respectively. Analysis of the protein content of individual

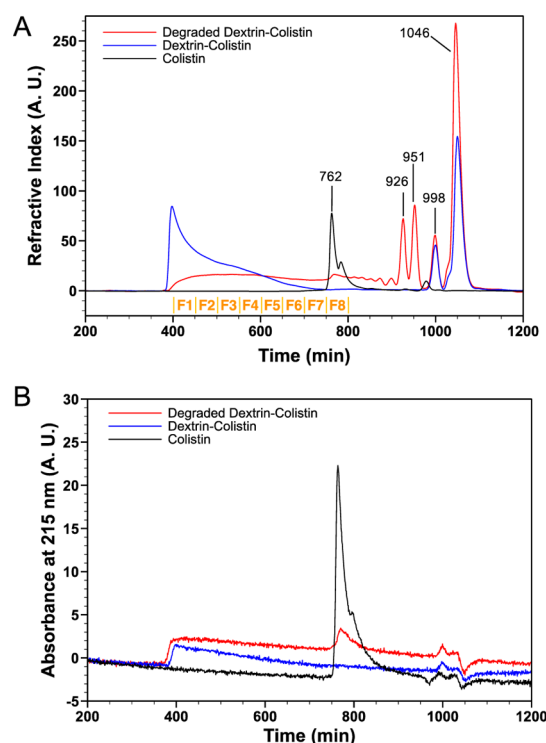


**Figure 2.** SEC chromatograms of colistin (black), dextrin–colistin conjugate (blue), and  $\alpha$ -amylase-treated (48 h at 37 °C) dextrin–colistin conjugate (red) by (A) RI detection and (B) UV detection ( $\lambda = 215$  nm). Collected fractions are shown in orange.

fractions revealed that fraction F8 (750–800 min retention time) contained the highest amount of colistin (38.8% w/w) compared to fractions F1–7 (400–750 min retention time, 2.1–5.5% w/w) (Table 1).

**Table 1. Protein Content and Antimicrobial Activity (Mode MIC,  $n = 3$ ) of Colistin Sulfate and Collected Fractions<sup>a</sup>**

fractions	protein content (% w/w)	MIC ( $\mu\text{g/mL}$ )
F1	2.1	4
F2	3.2	4
F3	2.9	8
F4	3.2	8
F5	3.4	4
F6	3.9	4
F7	5.5	2
F8	38.8	0.25
colistin	100	$1.95 \times 10^{-3}$

<sup>a</sup>Data is expressed as mode ( $n = 3$ ); MIC value represents equivalent colistin base concentration of fractions.

LC–mass spectrometry (MS) analysis revealed distinct structural differences between individual fractions and unmodified colistin (Table S2). Figure 3 illustrates ultra-performance liquid chromatography (UPLC) chromatograms and the corresponding mass spectra are shown in Figures S2–S5. Colistin’s UPLC chromatogram revealed two main peaks at 5.6 and 6.4 min, corresponding to colistin B and colistin A, respectively (Figure 3A). The chromatogram for fraction F8 contained a peak at 1.2 min, corresponding to oligosaccharides with DP 7–13 (1200–2100 g/mol) (Figure 3B). MS analysis of the peak revealed an intense peak at  $m/z$  839.22,

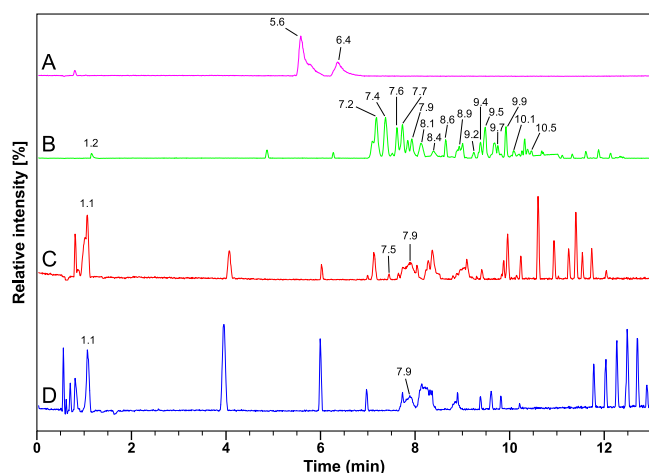


**Figure 3.** UPLC–QTOF–MS chromatograms (base peak intensity) of (A) colistin (10  $\mu\text{g/mL}$ ), (B) F8 (1 mg/mL), (C) F7 (1 mg/mL), and (D) F6 (1 mg/mL).

corresponding to an oligosaccharide with DP10 (Figure S3). In addition, the UPLC chromatogram of fraction F8 revealed multiple peaks, corresponding to colistin A and B attached to one linker  $\pm \text{H}_2\text{O}$  (7.2–8.6 min) and colistin A and B bound to two linkers  $-1$  or  $2 \text{H}_2\text{O}$  (8.9–10.4 min) (Figure 3B). Colistin A and B bound to two linkers without the loss of  $\text{H}_2\text{O}$  were not observed. Interestingly, peaks corresponding to the same molecular mass were observed at different retention times. The UPLC chromatogram for fraction F7 contained a peak at 1.1 min, corresponding to dehydrated oligosaccharides with DP 7–18 (1200–2900 g/mol) (Figure 3C). The MS analysis of the peak revealed the most intense peak at  $m/z$  1135.38, which corresponded to an oligosaccharide with DP14. In addition, peaks in the UPLC chromatogram between 7.5 and 7.9 min were observed, which corresponded to colistin B attached to 1–6 glucose units via a single linker  $\pm \text{H}_2\text{O}$ . Similarly to fractions F7 and F8, the UPLC chromatogram for fraction F6 contained a peak at 1.1 min, which corresponded to oligosaccharides with DP 13–22 (2100–3600 g/mol) (Figure 3D). The most intense peak by MS was detected at  $m/z$  1468.44, corresponding to DP18. A peak was also observed at 7.9 min, which corresponded to colistin B attached to 6–8 glucose units via a single linker and colistin A attached to 6–13 glucose units via a single linker. Sharp peaks observed between 3.5 and 6.5 min and above 9.5 min were impurities.

LC–MS analysis of unfractionated amylase-degraded dextrin–colistin conjugates with different degrees of succinylation (1.0, 2.5, and 7.5 mol %) revealed structural differences in released species (Figures S6 and S7, Table S3). Whereas the UPLC chromatogram for dextrin–colistin conjugates containing 1.0 mol % succinylated dextrin contained considerably more colistin A and B bound to only one linker, the UPLC chromatogram for the degraded conjugate containing 2.5 mol % succinylated dextrin revealed peaks corresponding to an almost equal proportion of colistin A and B bound to one (6.8–8.8 min) or two (8.8–11 min) linkers  $-1$  to  $2 \text{H}_2\text{O}$ . Smaller peaks corresponding to colistin A and B bound to 3 linkers  $-1$  to  $3 \text{H}_2\text{O}$  (11–13.4 min) were also observed. When the degree of dextrin succinylation was increased to 7.5 mol %, the intensity of peaks corresponding to colistin A and B bound to 2 or 3 linkers increased. This was mirrored by a decrease in the intensity of peaks corresponding to colistin A

and B with a single linker attached. In all cases, the maximum number of water molecules lost from the species was equal to the number of linkers attached to colistin; species with the greatest loss of water appeared later in the UPLC chromatogram.

**3.2. Biological Activity of Degraded Fractions.** All of the fractions analyzed exhibited lower antimicrobial activity than unmodified colistin (7–12 log-fold reduction in MIC), which varied between fractions. Antimicrobial activity was significantly higher for fraction F8, corresponding to fully unmasked colistin, than fractions corresponding to colistin with oligosaccharide chains attached (up to 5 log-fold reduction in MIC) (Table 1). The MIC value of the intact conjugate was  $2 \mu\text{g/mL}$ , which is equivalent to the MIC of the bound fractions (from F1 to F7). Whilst fraction F8 (at 1/4 MIC,  $0.0625 \mu\text{g/mL}$  colistin equiv) significantly delayed *E. coli* growth (by up to 10 h), fractions F6 and F7 showed limited effect on bacterial growth, even at 1/2 MIC (1 and  $2 \mu\text{g/mL}$  colistin equiv, respectively) (Figure 4). Bacterial lag time in the

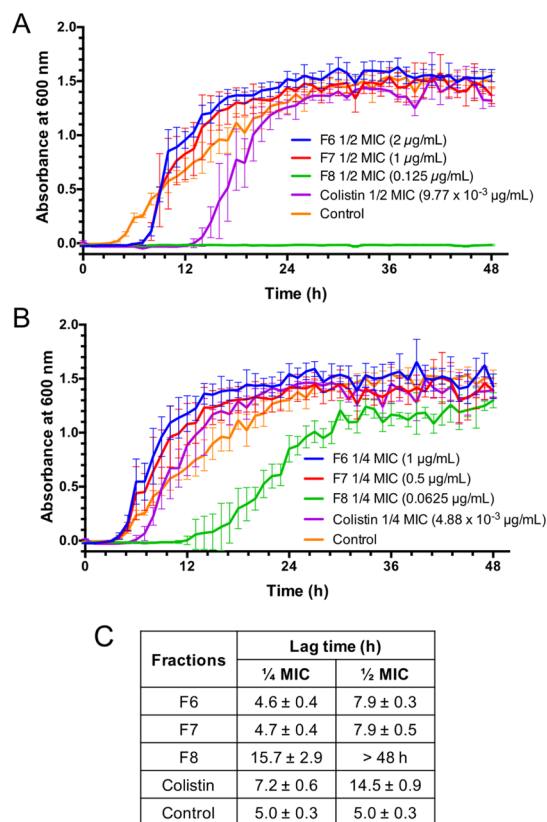


**Figure 4.** Bacterial growth curves for *E. coli* (48 h) in the presence of colistin sulfate and fractions F6, F7, and F8 at (A) 1/2 MIC and (B) 1/4 MIC (colistin base) (mean  $\pm$  SD;  $n = 3$ ). Corresponding lag times are indicated next to the figures. Panel (C) shows bacterial growth lag time, determined using an absorbance threshold of 0.1.

presence of colistin at 1/4 and 1/2 MIC ( $4.88 \times 10^{-3}$  and  $9.77 \times 10^{-3} \mu\text{g/mL}$  colistin equiv, respectively) was at least half that of bacteria grown in the presence of fraction F8 at 1/4 and 1/2 MIC (0.0625 and  $0.125 \mu\text{g/mL}$  colistin equiv, respectively) (Figure 4c). Observations in the planktonic culture systems were reflected in the effects of the fractions in bacterial biofilm systems. Fraction F8, at  $2\times$  MIC ( $0.5 \mu\text{g/mL}$  colistin equiv), effectively inhibited biofilm formation (Figure 5A). COMSTAT analysis of CLSM images revealed that this was

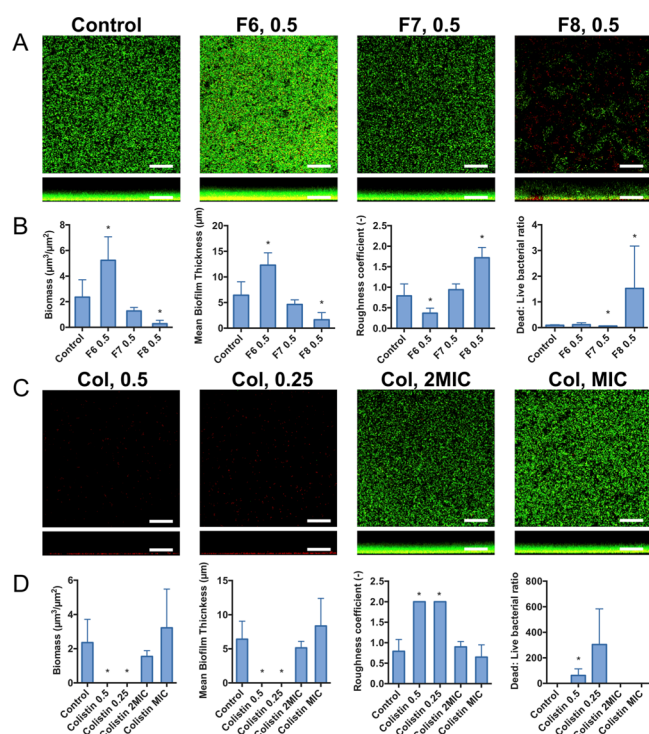


**Figure 5.** Biofilm formation assay showing LIVE/DEAD (green and red colors, respectively) stained CLSM images of *E. coli* biofilms (aerial and side view, scale bar = 40  $\mu\text{m}$ ) grown for 24 h in the presence of (A) fractions F6, F7, and F8 at 0.5  $\mu\text{g}/\text{mL}$  colistin base (equivalent to 2 $\times$  fraction F8's MIC) and (C) colistin sulfate at 0.25 and 0.5  $\mu\text{g}/\text{mL}$  colistin base, MIC and 2 $\times$  MIC. COMSTAT image analysis of biofilm CLSM z-stack images for (B) fractions and (D) colistin sulfate. Data represent mean  $\pm$  SD;  $n = 3$ . Significant difference is indicated by \*, where  $*p < 0.05$ , compared to untreated control.

associated with a significant reduction in biofilm biomass and thickness and a significant increase in roughness coefficient and bacterial cell death ( $p < 0.05$ , vs control; Figure 5B). Whereas fraction F7, at the same concentration, had no significant effect on biofilm formation, fraction F6 caused a significant increase in biofilm thickness and biomass ( $p < 0.05$ , vs control). When biofilms were grown in the presence of fractions at the MIC observed for F8 (0.25  $\mu\text{g}/\text{mL}$  colistin equiv), no significant effect on biofilm formation was observed in the presence of fractions F8 and F7, whereas treatment with fraction F6 caused a significant increase in biofilm biomass and thickness, mirrored by a decrease in roughness coefficient (Figure S8) ( $p < 0.05$ , vs control). In comparison, colistin at 0.25 and 0.5  $\mu\text{g}/\text{mL}$  (equivalent to fraction F8's MIC and 2 $\times$  MIC, respectively) caused complete inhibition of biofilm formation, whereas no effect on biofilm formation was observed when biofilms were grown at 0.002 and 0.004  $\mu\text{g}/\text{mL}$  (equivalent to colistin's MIC and 2 $\times$  MIC) (Figure 5C,D). Although antibacterial activity of the fully unmasked colistin was lower than the parent drug, in vitro cytotoxicity of fraction F8 was statistically less cytotoxic than both, unmodified colistin and intact dextrin–colistin conjugate in human kidney cells (Figure 6).

#### 4. DISCUSSION

In the last decades, biodegradable polymers have grown in popularity because of their ability to reduce the bioactive's

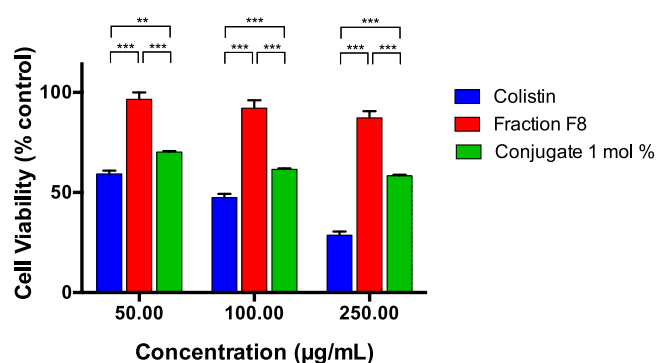


**Figure 6.** In vitro cytotoxicity of colistin sulfate, fraction F8, and intact dextrin–colistin conjugate (1 mol % succinylation). Cell viability was assessed by MTT assay of HK-2 cells (72 h incubation) at 50, 100, and 250  $\mu\text{g}/\text{mL}$  colistin base. Data are expressed as mean % untreated control  $\pm$  SEM,  $n = 18$ . Significant difference is indicated by \*, where  $**p < 0.01$  and  $***p < 0.001$ . For the conjugate, errors bars are too small to be visible.

antigenicity, extend circulatory half-life, and release the payload by degradation of the polymer at the target site.<sup>22–24</sup> Biodegradable polymers have the added advantage of enabling the use of much larger polymers because they are not limited to the renal threshold. Our previous studies, using dextrin–colistin conjugates, suggested that colistin's antibacterial activity is greatest when it was attached to shorter chains of dextrin with minimal modification;<sup>11</sup> however, the composition of the active species and the extent to which the polymer must be degraded to restore biological activity has not been defined in any studies relating to PUMPT.<sup>12</sup> An accurate definition of the “bound” and “free” species and identification of the structure–activity relationship are needed to develop and validate a chromatographic detection method to assess the pharmacokinetics and tissue distribution of dextrin–colistin conjugates. In previous studies, a colistin enzyme-linked immunosorbent assay kit was used to measure the pharmacokinetics; however, this method is unable to distinguish between “free” (active) and dextrin-bound (inactive) colistin.<sup>11</sup> In this study, fractionation of degraded dextrin–colistin conjugate by SEC followed by analysis using LC–MS and biological assays has been used to specifically determine the molecular structure of the active species.

**4.1. Chemical Characterization.** SEC-RI of the dextrin–colistin conjugate after amylase unmasking was successfully used to obtain fractions containing saccharides and colistin-based species with different molecular weights. Characterization of the molecular structure of low molecular weight derivatized peptides and conjugates is complex, necessitating the use of highly sensitive detection methods such as MS.<sup>25</sup> Because interpretation of MS data requires deconvolution of molecular fragments, in these studies, LC–MS was only performed on fractions corresponding to lower molecular weight species. LC was employed instead of direct injection as a separation of colistin-based species from released saccharides would make identification of the species more straightforward. Analysis of fraction F8 revealed a range of colistin-containing species, reflecting the heterogeneous composition of the conjugates due to nonspecific binding of dextrin to the 5 amino groups of colistin. This is also witnessed by the presence of peaks with different retention times corresponding to structures with the same molecular mass. This has been described previously; poly(ethylene glycol) (PEG)–protein

positional isomers and multiple PEGylated products are common, resulting from “nonselective” conjugation to several nucleophilic groups (e.g., lysine residues and terminal amine) on the protein.<sup>26,27</sup> This has led to researchers exploring site-selective conjugation methods.<sup>28,29</sup>

The presence of linkers attached to colistin’s amino groups increased its hydrophobicity. Thus, the species with more linkers attached appeared later in the UPLC chromatogram. Here, we showed that with increasing degree of succinylation, the number of linkers bound to colistin also increased. Previously, we used a ninhydrin assay to quantify the number of free amino groups following conjugation, which estimated that each colistin molecule was attached to dextrin via  $\sim 3$   $\text{NH}_2$  groups, regardless of the succinylation rate.<sup>11</sup> However, this method is unlikely to be as precise as LC–MS used here. Typically, increasing the extent of bioactive modification will reduce the bioactive’s antigenicity and extend its circulation half-life; however, this may be accompanied by a loss of the bioconjugate’s pharmacological activity.<sup>30</sup> Our observations here may explain the reduced antimicrobial activity of conjugates containing dextrans with a higher degree of succinylation, observed in our previous studies,<sup>11</sup> as well as that of other researchers.<sup>12</sup>

High-performance LC has previously been used to investigate the stability of commercial forms of the colistin prodrug, CMS, which readily undergoes random hydrolysis of the five sulfomethyl groups in aqueous solutions, resulting in up to 32 products.<sup>31–33</sup> In the same way as dextrin conjugation decreases colistin’s *in vitro* antibacterial potency, so too does sulfomethylation.<sup>34–36</sup> CMS is an inactive prodrug of colistin.<sup>37</sup> However, although amylase-triggered release of colistin released up to 80% free drug after 24 h *in vitro*,<sup>11</sup> conversion efficiency of CMS to colistin in the same period varies from 23 to 80% *in vitro* (in water, phosphate buffer and human plasma at 37 °C),<sup>11,31</sup> whereas only 30% of the prodrug is converted to colistin *in vivo*, as the remaining 70% of the CMS dose administered is excreted intact in the urine.<sup>31</sup> In contrast, colistin is not cleared renally and dextrin–colistin conjugates have demonstrated an extended plasma half-life following IV administration to rats.<sup>11</sup>

**4.2. Biological Activity.** Colistin is a highly potent antibiotic that has retained activity against most Gram-negative MDR strains.<sup>38–41</sup> In previous studies, MIC assays showed greater antimicrobial activity from dextrin–colistin conjugates containing colistin with fewer and shorter chains of minimally modified dextrin attached.<sup>11</sup> Similarly, Zhu et al. observed reduced antibiotic activity from bi-PEGylated colistin, compared to the mono-PEGylated antibiotic, which was attributed to the former’s larger molecular weight and slower colistin release rate.<sup>42</sup> Previously, pre-incubation of dextrin–colistin conjugates with physiological concentrations of amylase only reduced the MIC value by 1 log-fold, compared to the untreated conjugate;<sup>11</sup> however, these studies used a crude mixture of degraded conjugate, composed of a heterogeneous mixture of differentially degraded conjugates, which may mask the effect of the active species. Indeed, these studies showed a clear distinction in antimicrobial activity of fraction F8 and the larger fractions of degraded conjugate (which had an equivalent MIC to the intact dextrin–colistin), suggesting that complete degradation of dextrin is required to reinstate maximal antibiotic activity. Chemical characterization of fraction F8 showed that colistin retained a linker group attached to it, even after complete polymer degradation. This is

in contrast to CMS, where complete hydrolysis of all of the sulfomethyl groups forms the parent drug, colistin. Because colistin’s interaction with anionic lipopolysaccharide molecules on the outer membrane of Gram-negative bacteria is mediated via its 5 amine groups<sup>43</sup> and dextrin is conjugated to colistin via at least one of these groups, it is not surprising that the antibacterial activity is reduced by the presence of a linker group at this site. Interestingly, of the 10 novel polymyxin derivatives that have been shown to be more effective than conventional polymyxins in animal infection models, 8 of them retain all five Dab residues, confirming the importance of the positively charged amine groups for antimicrobial activity.<sup>44</sup> A similar inability to completely recover the bioactive’s biological activity (following enzymatic polymer degradation) has also been observed when hyaluronan was conjugated to EGF, using similar conjugation chemistry;<sup>13</sup> a finding attributed to the presence of oligosaccharides attached to the lysine residue close to EGF’s receptor-binding domain. In previous antibiotic conjugation models, in an attempt to maximize antibiotic activity, Zhu et al. used a labile ester linker in their mono-PEGylated colistin to facilitate release of drug that was chemically identical to unmodified colistin and retained similar activity to the native peptide.<sup>42</sup> Here, treatment with fraction F6 counter-intuitively induced significant biofilm growth, presumably because of the bacteria using the longer oligosaccharide chains as a carbon- and energy source.

In practice, systemic administration of colistin may be restricted by dose-limiting nephrotoxicity, which occurs due to reabsorption and accumulation of colistin in renal tubular cells.<sup>11</sup> Previous studies showed that dextrin conjugation reduced colistin’s *in vitro* cytotoxicity toward human kidney proximal tubule (HK-2) cells, with around a four–fivefold improved  $\text{IC}_{50}$  concentration.<sup>11</sup> Even after amylase-unmasking of dextrin–colistin conjugates, cytotoxicity remained similar to the intact conjugate and less than colistin sulfate. Given the heterogeneous composition of this crude mixture, it was important in the current study to test the cytotoxicity of the individual fractions. Whilst the finding that fraction F8 was significantly less toxic *in vitro* than the intact dextrin–colistin conjugate appeared surprising, Zhu et al. demonstrated that colistin attached to a single PEG chain failed to induce histological renal damage *in vivo* at 40 mg colistin equiv/kg, but the presence of 2 PEG chains, however, resulted in renal tubular injury.<sup>42</sup> The authors attributed this difference in nephrotoxicity to the complex and different renal handling mechanisms of the mono- and di-PEGylated colistin. Here, the reduced toxicity observed in fraction F8, compared to the intact dextrin–colistin conjugate, may reflect altered uptake and accumulation by HK-2 cells because of the oligosaccharides attached to colistin.

**4.3. Future Perspectives.** Our ultimate goal is to develop and validate a chromatographic detection method to study degradation and biodistribution of dextrin–colistin conjugates following *in vivo* administration by analysis of serum and other biological samples (e.g., macerated organs). Method development is ongoing but challenging because the chemical diversity of the released species precludes the use of reversed-phase separation and the low absorbance of colistin necessitates the use of a derivatization method that will not be affected by residual saccharide moieties. The results of these structure–activity relationship studies demonstrate that complete unmasking of colistin is required for maximum antibiotic activity. Because the smallest fractions may not localize as

efficiently to sites of infection by the EPR effect and are likely to be cleared faster from the body, ideally, unmasking should occur predominantly at the target site. We have previously shown that the  $\alpha$ -amylase activity is significantly higher in infected wound fluid compared to that in patient-matched serum (408.4 and 60.0 IU/L, respectively),<sup>15</sup> which suggests that this could be feasible. Ongoing studies are developing an in vivo mouse model to test this hypothesis and quantify the amount of “free”/active and “bound”/inactive colistin in biological samples.

## 5. CONCLUSIONS

This study highlights the importance of defining the structure–antimicrobial activity relationship for novel antibiotic derivatives. Here, we have demonstrated that the presence of functional groups attached to colistin significantly affects its biological activity, and this effect can be minimized (but not fully reversed) by enzymatic degradation of the polymer. LC–MS is a valuable tool for characterizing conjugation patterns, which can aid in the design of biodegradable polymer–antibiotic conjugates, as well as for studying drug distribution and disposition in vivo.

## ■ ASSOCIATED CONTENT

### 📄 Supporting Information

The Supporting Information is available free of charge on the ACS Publications website at DOI: 10.1021/acs.molpharmaceut.9b00393.

Characteristics of dextrin–colistin conjugates, HPAEC–PAD analysis, identification of the detected species from UPLC–QTOF–MS analysis, QTOF–MS spectra, and chromatograms and CLSM images (PDF)

## ■ AUTHOR INFORMATION

### Corresponding Author

\*E-mail: [FergusonEL@cardiff.ac.uk](mailto:FergusonEL@cardiff.ac.uk).

### ORCID

Mathieu Varache: 0000-0001-7166-2253

Olav A. Aarstad: 0000-0003-3671-9060

### Author Contributions

E.L.F., D.W.T., and M.V. conceived and designed the work. M.V. devised experiments, performed data collection, and data analysis. L.C.P. performed CLSM analysis of bacterial biofilms. O.A.A. performed SEC fractionation and HPAEC–PAD analysis. T.L.W. and M.N.W. assisted in LC–MS analysis and data interpretation. All authors contributed to data interpretation. E.L.F. and M.V. drafted the manuscript, and all authors reviewed and approved the manuscript.

### Notes

The authors declare no competing financial interest.

## ■ ACKNOWLEDGMENTS

This work was supported by a research grant from the UK Medical Research Council (MR/N023633/1).

## ■ REFERENCES

- (1) Shlaes, D. M. *Antibiotics: The Perfect Storm*; Springer Netherlands, 2010.
- (2) Tacconelli, E.; Carrara, E.; Savoldi, A.; Harbarth, S.; Mendelson, M.; Monnet, D. L.; Pulcini, C.; Kahlmeter, G.; Kluytmans, J.; Carmeli, Y.; et al. Discovery, Research, and Development of New Antibiotics:

The WHO Priority List of Antibiotic-Resistant Bacteria and Tuberculosis. *Lancet Infect. Dis.* **2018**, *18*, 318–327.

- (3) Michalopoulos, A. S.; Tsiodras, S.; Rellos, K.; Mentzelopoulos, S.; Falagas, M. E. Colistin Treatment in Patients with ICU-Acquired Infections Caused by Multiresistant Gram-Negative Bacteria: The Renaissance of an Old Antibiotic. *Clin. Microbiol. Infect.* **2005**, *11*, 115–121.

- (4) Cheng, C.-Y.; Sheng, W.-H.; Wang, J.-T.; Chen, Y.-C.; Chang, S.-C. Safety and Efficacy of Intravenous Colistin (Colistin Methanesulphonate) for Severe Multidrug-Resistant Gram-Negative Bacterial Infections. *Int. J. Antimicrob. Agents* **2010**, *35*, 297–300.

- (5) Fair, R. J.; Tor, Y. Antibiotics and Bacterial Resistance in the 21st Century. *Perspect. Med. Chem.* **2014**, *6*, 25–64.

- (6) Falagas, M.; Kasiakou, S. Toxicity of Polymyxins: A Systematic Review of the Evidence from Old and Recent Studies. *Crit. Care* **2006**, *10*, R27.

- (7) Ordooei Javan, A.; Shokouhi, S.; Sahraei, Z. A Review on Colistin Nephrotoxicity. *Eur. J. Clin. Pharmacol.* **2015**, *71*, 801–810.

- (8) Elverdam, I.; Larsen, P.; Lund, E. Isolation and Characterization of Three New Polymyxins in Polymyxins B and E by High-Performance Liquid Chromatography. *J. Chromatogr. A* **1981**, *218*, 653–661.

- (9) Orwa, J. A.; Van Gerven, A.; Roets, E.; Hoogmartens, J. Development and Validation of a Liquid Chromatography Method for Analysis of Colistin Sulphate. *Chromatographia* **2000**, *51*, 433–436.

- (10) Decolin, D.; Leroy, P.; Nicolas, A.; Archimbault, P. Hyphenated Liquid Chromatographic Method for the Determination of Colistin Residues in Bovine Tissues. *J. Chromatogr. Sci.* **1997**, *35*, 557–564.

- (11) Ferguson, E. L.; Azzopardi, E.; Roberts, J. L.; Walsh, T. R.; Thomas, D. W. Dextrin–Colistin Conjugates as a Model Bioresponsive Treatment for Multidrug Resistant Bacterial Infections. *Mol. Pharm.* **2014**, *11*, 4437–4447.

- (12) Duncan, R.; Gilbert, H. R. P.; Carbajo, R. J.; Vicent, M. J. Polymer Masked–Unmasked Protein Therapy. 1. Bioresponsive Dextrin–Trypsin and –Melanocyte Stimulating Hormone Conjugates Designed for  $\alpha$ -Amylase Activation. *Biomacromolecules* **2008**, *9*, 1146–1154.

- (13) Ferguson, E. L.; Alshame, A. M. J.; Thomas, D. W. Evaluation of Hyaluronic Acid–Protein Conjugates for Polymer Masked–Unmasked Protein Therapy. *Int. J. Pharm.* **2010**, *402*, 95–102.

- (14) Talelli, M.; Vicent, M. J. Reduction Sensitive Poly(l-Glutamic Acid) (PGA)-Protein Conjugates Designed for Polymer Masked–Unmasked Protein Therapy. *Biomacromolecules* **2014**, *15*, 4168–4177.

- (15) Azzopardi, E. A.; Ferguson, E. L.; Thomas, D. W. Development and Validation of an In Vitro Pharmacokinetic/Pharmacodynamic Model To Test the Antibacterial Efficacy of Antibiotic Polymer Conjugates. *Antimicrob. Agents Chemother.* **2015**, *59*, 1837–1843.

- (16) Azzopardi, E. A.; Ferguson, E. L.; Thomas, D. W. The Enhanced Permeability Retention Effect: A New Paradigm for Drug Targeting in Infection. *J. Antimicrob. Chemother.* **2013**, *68*, 257–274.

- (17) Hardwicke, J.; Ferguson, E.; Moseley, R.; Stephens, P.; Thomas, D.; Duncan, R. Dextrin–RhEGF Conjugates as Bioresponsive Nanomedicines for Wound Repair. *J. Control. Release* **2008**, *130*, 275–283.

- (18) Davies, D. Kinetics of Icodextrin. *Perit. Dial. Int.* **1994**, *14*, S45–S50.

- (19) Khan, S.; Tøndervik, A.; Sletta, H.; Klinkenberg, G.; Emanuel, C.; Onsoyen, E.; Myrvold, R.; Howe, R. A.; Walsh, T. R.; Hill, K. E.; et al. Overcoming Drug Resistance with Alginate Oligosaccharides Able To Potentiate the Action of Selected Antibiotics. *Antimicrob. Agents Chemother.* **2012**, *56*, S134–S141.

- (20) Jorgensen, J. H.; Turnidge, J. D. Susceptibility Test Methods: Diffusion and Disk Diffusion Methods\*. *Manual of Clinical Microbiology*; American Society of Microbiology, 2015; pp 1253–1273.

- (21) Heydorn, A.; Nielsen, A. T.; Hentzer, M.; Sternberg, C.; Givskov, M.; Ersbøll, B. K.; Molin, S. Quantification of Biofilm Structures by the Novel Computer Program COMSTAT. *Microbiology* **2000**, *146*, 2395–2407.

- (22) Basu, A.; Kunduru, K. R.; Abtew, E.; Domb, A. J. Polysaccharide-Based Conjugates for Biomedical Applications. *Bioconjug. Chem.* **2015**, *26*, 1396–1412.
- (23) Qi, Y.; Chilkoti, A. Protein–Polymer Conjugation—Moving beyond PEGylation. *Curr. Opin. Chem. Biol.* **2015**, *28*, 181–193.
- (24) Pasut, G. Polymers for Protein Conjugation. *Polymers* **2014**, *6*, 160–178.
- (25) Pollock, J. F.; Ashton, R. S.; Rode, N. A.; Schaffer, D. V.; Healy, K. E. Molecular Characterization of Multivalent Bioconjugates by Size-Exclusion Chromatography with Multiangle Laser Light Scattering. *Bioconjug. Chem.* **2012**, *23*, 1794–1801.
- (26) Wang, Y.-S.; Youngster, S.; Bausch, J.; Zhang, R.; McNemar, C.; Wyss, D. F. Identification of the Major Positional Isomer of Pegylated Interferon Alpha-2b. *Biochemistry* **2000**, *39*, 10634–10640.
- (27) Dhalluin, C.; Ross, A.; Leuthold, L.-A.; Foser, S.; Gsell, B.; Müller, F.; Senn, H. Structural and Biophysical Characterization of the 40 kDa PEG–Interferon- $\alpha$ 2a and Its Individual Positional Isomers. *Bioconjug. Chem.* **2005**, *16*, 504–517.
- (28) Hu, Q.-Y.; Berti, F.; Adamo, R. Towards the next Generation of Biomedicines by Site-Selective Conjugation. *Chem. Soc. Rev.* **2016**, *45*, 1691–1719.
- (29) Pasut, G.; Veronese, F. M. State of the Art in PEGylation: The Great Versatility Achieved after Forty Years of Research. *J. Control. Release* **2012**, *161*, 461–472.
- (30) Clark, R.; Olson, K.; Fuh, G.; Marian, M.; Mortensen, D.; Teshima, G.; Chang, S.; Chu, H.; Mukku, V.; Canova-Davis, E.; et al. Long-Acting Growth Hormones Produced by Conjugation with Polyethylene Glycol. *J. Biol. Chem.* **1996**, *271*, 21969–21977.
- (31) Li, J.; Milne, R. W.; Nation, R. L.; Turnidge, J. D.; Coulthard, K. Stability of Colistin and Colistin Methanesulfonate in Aqueous Media and Plasma as Determined by High-Performance Liquid Chromatography. *Antimicrob. Agents Chemother.* **2003**, *47*, 1364–1370.
- (32) Post, T. E.; Kamerling, I. M. C.; van Rossen, R. C. J. M.; Burggraaf, J.; Stevens, J.; Dijkmans, A. C.; Heijerman, H. G. M.; Touw, D. J.; van Velzen, A. J.; Wilms, E. B. Colistin Methanesulfonate Infusion Solutions Are Stable over Time and Suitable for Home Administration. *Eur. J. Hosp. Pharm.* **2018**, *25*, 337–339.
- (33) Wallace, S. J.; Li, J.; Rayner, C. R.; Coulthard, K.; Nation, R. L. Stability of Colistin Methanesulfonate in Pharmaceutical Products and Solutions for Administration to Patients. *Antimicrob. Agents Chemother.* **2008**, *52*, 3047–3051.
- (34) Barnett, M.; Bushby, S. R. M.; Wilkinson, S. Sodium Sulphomethyl Derivatives of Polymyxins. *Br. J. Pharmacol. Chemother.* **1964**, *23*, 552–574.
- (35) Beveridge, E. G.; Martin, A. J. Sodium Sulphomethyl Derivatives of Polymyxins. *Br. J. Pharmacol. Chemother.* **1967**, *29*, 125–135.
- (36) Schwartz, B. S.; Warren, M. R.; Barkley, F. A.; Landis, L. Microbiological and Pharmacological Studies of Colistin Sulfate and Sodium Colistinmethanesulfonate. *Antibiot. Annu.* **1959**, *7*, 41–60.
- (37) Bergen, P. J.; Li, J.; Rayner, C. R.; Nation, R. L. Colistin Methanesulfonate Is an Inactive Prodrug of Colistin against *Pseudomonas Aeruginosa*. *Antimicrob. Agents Chemother.* **2006**, *50*, 1953–1958.
- (38) Li, J.; Nation, R. L.; Turnidge, J. D.; Milne, R. W.; Coulthard, K.; Rayner, C. R.; Paterson, D. L. Colistin: The Re-Emerging Antibiotic for Multidrug-Resistant Gram-Negative Bacterial Infections. *Lancet Infect. Dis.* **2006**, *6*, 589–601.
- (39) Nation, R. L.; Li, J. Colistin in the 21st Century. *Curr. Opin. Infect. Dis.* **2009**, *22*, 535–543.
- (40) Li, J.; Nation, R. L.; Milne, R. W.; Turnidge, J. D.; Coulthard, K. Evaluation of Colistin as an Agent against Multi-Resistant Gram-Negative Bacteria. *Int. J. Antimicrob. Agents* **2005**, *25*, 11–25.
- (41) Biswas, S.; Brunel, J.-M.; Dubus, J.-C.; Reynaud-Gaubert, M.; Rolain, J.-M. Colistin: An Update on the Antibiotic of the 21st Century. *Expert Rev. Anti Infect. Ther.* **2012**, *10*, 917–934.
- (42) Zhu, C.; Schneider, E. K.; Wang, J.; Kempe, K.; Wilson, P.; Velkov, T.; Li, J.; Davis, T. P.; Whittaker, M. R.; Haddleton, D. M. A Traceless Reversible Polymeric Colistin Prodrug to Combat Multi-drug-Resistant (MDR) Gram-Negative Bacteria. *J. Controlled Release* **2017**, *259*, 83.
- (43) Vaara, M. Agents That Increase the Permeability of the Outer Membrane. *Microbiol. Rev.* **1992**, *56*, 395–411.
- (44) Vaara, M. New Polymyxin Derivatives That Display Improved Efficacy in Animal Infection Models as Compared to Polymyxin B and Colistin. *Med. Res. Rev.* **2018**, *38*, 1661–1673.